Journal of Nuclear Materials 392 (2009) 171–175

Contents lists available at ScienceDirect

Journal of Nuclear Materials

journal homepage: www.elsevier.com/locate/jnucmat

Nitration by a simulated fuel technique for nitride fuel re-fabrication

Young.-Woo Lee *, Ho Jin Ryu, Jae Won Lee, Jung Won Lee, Geun Il Park

Korea Atomic Energy Research Institute, P.O. Box 105, Yuseong, Daejeon 305-600, Republic of Korea

ABSTRACT

Nitration reaction of a spent nuclear oxide fuel through a carbothermic reduction and the change in thermal conductivity of the resultant nitride specimens were investigated by a simulated fuel technique for use in nitride fuel re-fabrication from spent oxide fuel. The simulated spent oxide fuel was formed by compacting and sintering a powder mixture of UO_2 and stable oxide fission product impurities. It was pulverized by a 3-cycle successive oxidation–reduction treatment and converted into nitride pellet specimens through the carbothermic reduction. The rate of the nitration reaction of the simulated spent oxide fuel was decreased due to the fission product impurities when compared with pure uranium dioxide. The amount of Ba and Sr in the simulated spent oxide fuel was considerably reduced after the nitride fuel re-fabrication. The thermal conductivity of the nitride pellet specimen in the range 295–373 K was lower than that of the pure uranium nitride but higher than the simulated spent oxide fuel containing fission product impurities.

1. Introduction

Worldwide R&D activities in nuclear energy are currently focused on reduction and utilization of spent nuclear fuels for both a high level radioactive waste reduction and the production of energy. This is coordinated through joint international efforts such as the Generation IV International Forum (GIF) and the Global Nuclear Energy Partnership (GNEP). Technical issues concerning these joint efforts include a separation of the Minor Actinides (MAs: Am, Cm and Np) and their transmutation. These elements can be transmuted, preferably in a fast neutron system, for which non-oxide fuel materials are more advantageous than oxide in respect of their mutual miscibility and in-reactor fuel material performance. Currently, investigations for these innovative nuclear fuel materials are underway in several countries [1,2].

Generally, a nitride fuel demonstrates, as summarized and compared to other nuclear fuel materials in Table 1 [3], a high fuel material density, high melting point and high thermal conductivity, and good compatibility with Na coolant and stainless steel cladding. In addition, uranium and plutonium nitride fuels can form solid solutions with nitrides containing MAs. The nitride compounds of these elements are expected to be effectively utilized for the transmutation strategy in Liquid Metal Fast Breeder reactors as well as for Accelerator-Driven System fuel target materials [4,5]. One of the issues for these nitrides as fuel materials is the formation of radio-toxic C-14 by a (n, p) reaction and B-11 by a (n, α) reaction of N-14. B-11 has a high neutron absorption cross-section, and hence decreases the neutron economy of the reactor. This can be overcome by the use of N_2 gas enriched in N-15 isotope during the nitride fuel fabrication process. The enrichment of this isotope is currently being investigated [6,7]. Another technical solution can be the use of a pyrochemical process for the treatment of the spent fuel, in which N-15 can be readily recovered and recycled [8].

Review of work on nitride fuel materials and other fast reactor fuels has been well documented in papers by Matke [9] in the 1980s and Blank [10] in the 1990s, and later by international organizations, including the IAEA [11] and OECD/NEA [12] in the 2000s. However, compared with oxide fuels, the irradiation experience for nitride fuels has not achieved the level of a database for verification and validation of their in-reactor performance. Current interest in nitride fuel is focused on the fabrication and material properties of nitride fuel containing MAs as well as on the irradiation performance. This will require rather comprehensive irradiation tests in a dedicated nuclear system.

The fabrication process for nitride fuel established from earlier works has been applied for fabricating nitride fuel containing MAs [4]. The material properties are currently being investigated for in-reactor performance, including changes during irradiation [12]. One of the important issues is the selection of a fuel system, which must be based on the consideration of a fuel recycling mode with regard to the actinide inventory for a facility, the fabrication technology and the fuel design and its performance [13]. In this regard, one of the options for a fuel in a fast reactor system can be a ‘dirty nitride fuel’, containing not only MAs but also solid fission product elements, this fuel being converted from spent oxide fuels.

This work is part of a feasibility study for re-fabrication of nitride fuel by the use of the DUPIC fuel cycle technology concept [14]. This process is a dry processing technology concept for re-fabrication of spent oxide fuel. The nitration of spent oxide fuel

---

* Corresponding author. Tel.: +82 42 868 2129; fax: +82 42 868 4826.
E-mail address: ywlee@kaeri.re.kjr (Young.-Woo Lee).

0022-3115/$ - see front matter © 2009 Published by Elsevier B.V.
doi:10.1016/j.jnucmat.2009.03.042

Table 1
Comparison of material properties among oxide, carbide, nitride and metallic nuclear fuels [3].

	Oxide	Carbide	Nitride	Metallic alloy
Material	$(U_{0.8}Pu_{0.2})O_{1.97-1.98}$	$(U_{0.8}Pu_{0.2})C_{1.02-1.05}$	$(U_{0.8}Pu_{0.2})N_{1.0}$	U–20Pu–10Zr
Theoretical density (g/cm^3)	11.1	13.6	14.3	15.6
Heavy metal density (g/cm^3)	9.8	12.9	13.5	14.1
Thermal conductivity (W/mK) (773–1273 K)	2.5–5	15–21	14–22	18–25
Melting point (K)	3023	2709	3050	1428

material containing fission products through a carbothermic reduction was attempted and analyzed, from the material aspects, using a simulated fuel technique (SFT) with uranium oxide mixed with stable surrogate solid fission product oxides.

2. Experimental

A conventional powder-pellet route was adopted for the preparation of a simulated spent PWR oxide fuel, in which UO_2 powder was admixed and milled with selected stable fission product oxides, and compacted and sintered to a cylindrical pellet [15] to simulate burnup in a PWR. This simulation technique, which is sometimes used for estimating the properties and behavior of spent nuclear fuel materials [16], was used in this work for easy handling of experimental materials instead of using hot cells for the delicate and complicated handling of spent nuclear fuel materials.

Table 2
Chemical composition of simulated spent fuel.

Element	Stable oxide fission product surrogate	wt.%
Sr	SrO	0.053
Y	Y_2O_3	0.035
Zr	ZrO_2	0.284
Mo	MoO_3	0.253
Tc	RuO_2	0.059
Ru	RuO_2	0.166
Rh	Rh_2O_3	0.032
Pd	PdO	0.109
Ba	$BaCO_3$	0.146
La	La_2O_3	0.094
Ce	CeO_2	0.183
Pr	Nd_2O_3	0.086
Nd	Nd_2O_3	0.310
Sm	Nd_2O_3	0.068
U	UO_2	97.255
Np	CeO_2	0.035
Pu	CeO_2	0.722
Am	La_2O_3	0.071

Fig. 1 shows a schematic flow diagram for the spent nitride fuel sample preparation. Simulated spent oxide fuel powder with composition of its major fission products corresponding to a spent LWR fuel with a discharge burnup of 27,300 MWd/MtU and then 10-year storage was obtained by mixing UO_2 powder with fission product oxide additives. Eleven major oxides were selected as additives for simulating the fission products based on a calculation result by the ORIGEN-2 code [17], as shown in Table 2. In order to obtain sintered simulated spent oxide pellet specimens, the natural UO_2 powder was mixed with the stable fission product oxide powders with the weight fractions shown in Table 2. Wet attrition milling used methanol and alumina balls as milling media for 2 h at 200 rpm. The wet milled powder mixture was dried for 5 days at 313 K in a drying oven. The dried powder was mixed again with 0.2 wt% zinc stearate in a turbular mixer for 30 min. Then the powder was compacted with a pressure of 100 MPa to obtain compact specimens with a diameter of 10 mm, and subsequently sintered at 2023 K for 4 h in a H_2 atmosphere. This preparation method resulted in simulated spent oxide specimens with a solid solution of the stable oxides [15].

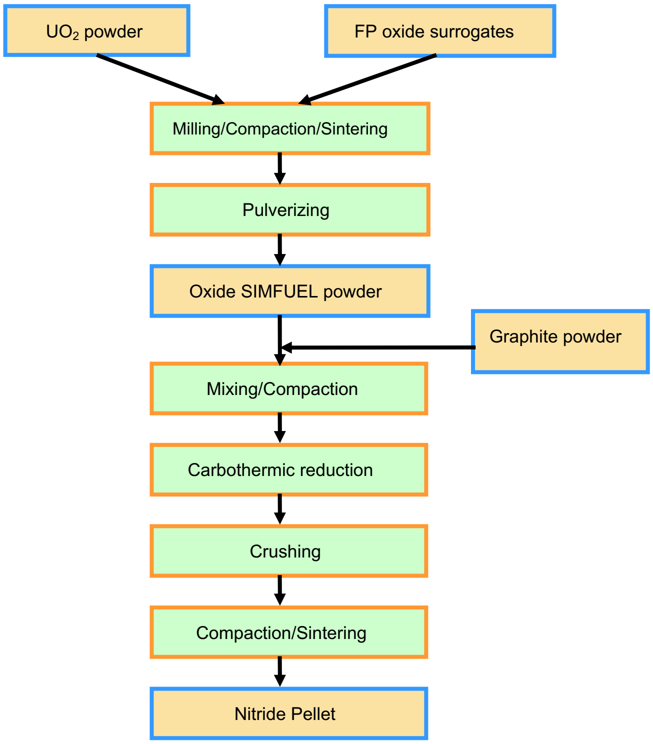

Fig. 1. Schematic flow diagram for simulated nitride specimen re-fabrication.

In order to fabricate the simulated nitride pellets specimens, the prepared simulated spent oxide fuel pellet specimens were first pulverized by means of the 3-cycle repetitive oxidation and reduction, at 723 K for 2 h in air for oxidation and 973 K for 7 h in an Ar-4 vol%H_2 gas mixture for reduction. This produced a sinterable solid solution powder (SSP). This SSP was then mixed with graphite powder in a turbular mixer to a ratio of C/(U+FP elements) of 2.2–2.5, compacted with a pressure of 100 MPa to prepare compact specimens with an average diameter of 13.2 mm and a height of about 3–4 mm, which were then heat-treated by two successive steps, at 1973 K in N_2 for 3 h and at 1923 K in N_2 and Ar–4 vol%H_2 gas mixture for 3 h, as shown in Fig. 2. The first step was a carbothermic reduction where the uranium oxide was reduced by the mixed graphite powder and reacted with N_2 gas to be converted to uranium nitride. For this reaction, flowing N_2 gas at 1000 cm^3/min was used at the reaction temperature of 1973 K for 3 h. The second step was the residual carbon removal step, where the N_2 reaction gas mixed with an Ar–4 vol%H_2 gas mixture was used and the specimens were heat-treated at 1923 K for 3 h. The overall general reaction equation for the nitride formation from uranium dioxide can be written as follows:

$$UO_2 + (2+n)C + 1/2N_2 + 2nH_2 \rightarrow UN + 2CO + nCH_4 \quad (1)$$

The steps in the nitride pellet preparation included crushing of the nitride pellets by use of a mortar, compacting the crushed powder at pressure of 300 MPa, and then sintering at 1973 K for 10 h in

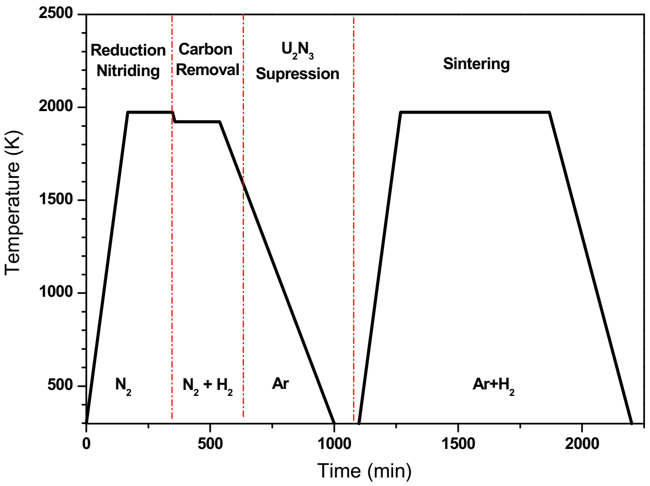

Fig. 2. Temperature profiles and atmosphere gases used during nitration through carbothermic reduction.

an Ar–4 vol%H_2 gas mixture to obtain re-fabricated nitride pellet specimens. The microstructure of the re-fabricated nitride pellet specimens was analyzed using an optical microscope. The nitride phase was analyzed by X-ray diffraction, and the density and thermal diffusivity of the nitride pellet specimens were measured by the water immersion method and a laser flash technique, respectively. Chemical analysis was also performed on the specimens before and after the nitration reaction to determine change in chemical composition of the re-fabricated nitride pellet specimens.

In addition to the nitride specimen preparation described above, the nitration behaviors of pure UO_2 and the simulated spent oxide were analyzed by TG/DTA (Thermo-Gravimetry/Differential Thermal Analysis) and compared. For these experiments, pure UO_2 powder and the SSP were, respectively, mixed with graphite powder in a turbular mixer to a ratio of C/(U+FP elements) of 2.2 and compacted with a pressure of 100 MPa. The atmosphere employed for the nitration behavior analysis by TG/DTA was N_2 gas; an Ar–4 vol%H_2 gas mixture was not included. This evaluated the nitration behavior of pure UO_2 and the simulated spent oxide specimens. The temperature of the reaction was fixed at 1773 K, which is lower than the temperature of the actual nitration reaction for the preparation of the re-fabricated nitride pellet specimens (1923 K), to examine the nitration reaction behavior.

3. Results and discussion

3.1. Nitration behavior analyzed by TGA

In order to prepare re-fabricated nitride pellet specimens, a TG experiment of the nitration reaction was attempted with pure UO_2 and the simulated spent oxide powders. Fig. 3 shows the TG analysis results of the carbothermic reduction, together with that of pure UO_2 for comparison. It can be noted in Fig. 3(a) that, for both specimens, the weight change during the carbothermic reaction is quite similar, with the only difference being in the time required for completion of the reaction. For the UO_2 specimen, the reaction required about 7 h whereas the simulated spent oxide specimen took about 9 h for completion of the nitration. This reveals that the fission product elements hinder the carbothermic reaction. Nitration of a simulated spent oxide by carbothermic reduction resulted in 18% radial shrinkage, 17% weight decrease and 52.5% TD (Theoretical Density). A weight decrease of 17% is similar to the theoretically calculated weight decrease of 15% when UO_2 is converted to UN. Fig. 3(b) shows the fraction of weight change during the nitration reaction of UO_2 and the simulated spent oxide specimens. The slope of the weight change fraction versus the reaction time of the simulated spent oxide specimen is lower than that of the pure UO_2 specimen, also indicating that the fission products hinder the nitration reaction. It is known [18] that the oxidation rate of spent oxide fuel decreases with increasing burn-up and hence, it can be expected that a higher burn-up spent oxide fuel requires a longer time for nitration. The weight increase at the end of a cooling in Fig. 3(a) indicates the formation of U_2N_3, a sesquinitride phase due to the N_2 gas atmosphere, which was confirmed by X-ray diffraction.

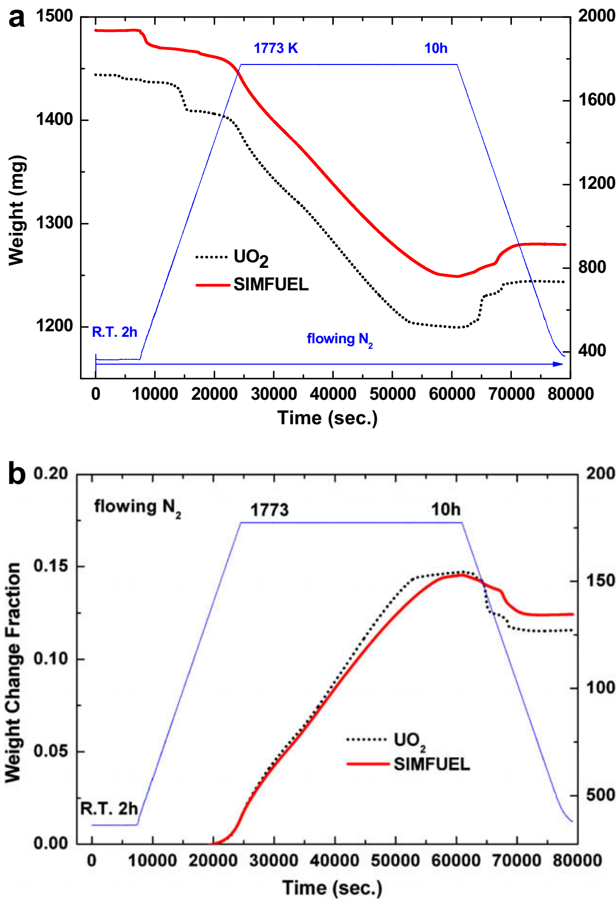

Fig. 3. Thermogravimetry results of carbothermic reductions of UO_2 and simulated spent oxide fuel. (a) Weight change and (b) weight change fraction during nitration reaction.

3.2. Characterization of the re-fabricated nitride specimen

The nitride fuel specimens re-fabricated from the simulated spent oxide fuel by using the process in Fig. 1 were characterized in terms of their phase identification by X-ray diffraction, density, thermal conductivity up to 373 K and compositional change by chemical analysis. Fig. 4 shows X-ray diffraction patterns of the nitride specimens. Fig. 4(a) is for the nitride specimen by nitration with a cooling step in Ar below 1673 K, which results in a UN-structured nitride formation, whereas Fig. 4(b) shows an X-ray diffraction pattern for U_2N_3-structured nitride formation caused by a cooling step in N_2 gas below 1673 K.

For examination of the influence of graphite addition to the initial powder mixture on the residual carbon content after the nitration reaction with the selected experimental conditions, three different specimens were prepared with C/(U+FP elements) ratios

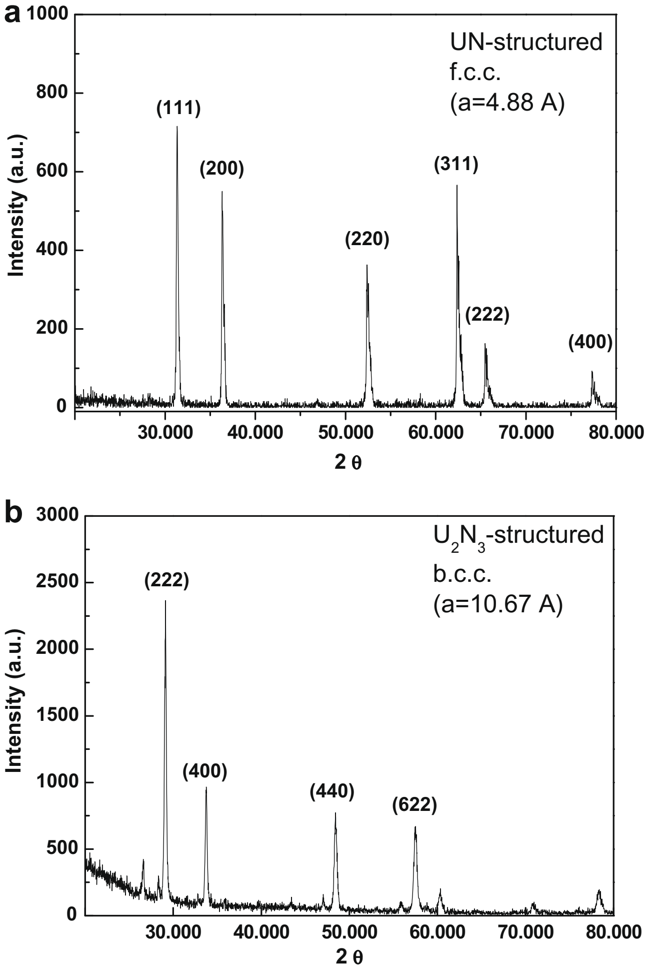

Fig. 4. XRD diffraction patterns of nitride powders; (a) UN structure and (b) U_2N_3 structure.

Table 3
Carbon content in nitride pellets after carbothermic reduction.

Initial C/(U+FP elements)	2.20	2.35	2.50
Residual carbon content (wt%)	0.854	1.661	2.037

Table 4
Chemical analysis for Ba and Sr in nitride fuel.

Specimen	Element	
	Ba (ppm)	Sr (ppm)
SIMFUEL	1080 ± 40	418 ± 20
Nitride	<5	<5

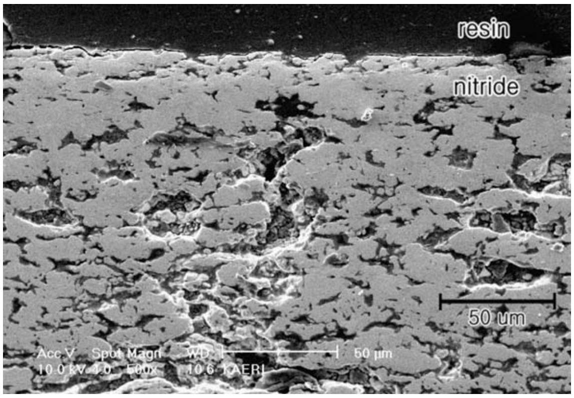

Fig. 5. Microstructure of re-fabricated nitride pellet using simulated spent oxide fuel.

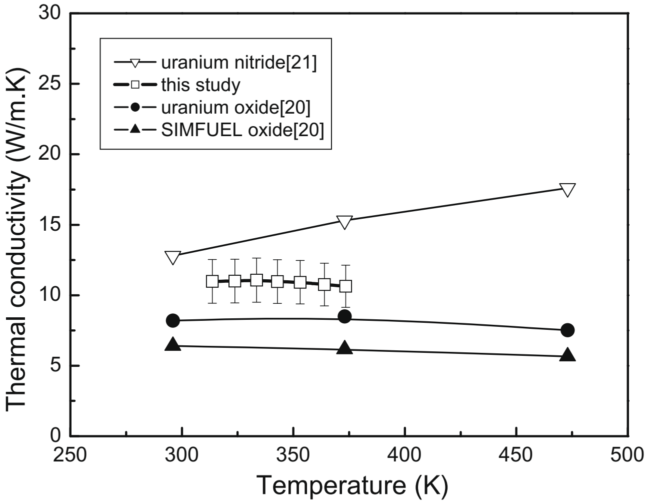

Fig. 6. Comparison of thermal conductivity of a simulated nitride with those for pure uranium nitride, uranium oxide and simulated spent oxide (SIMFUEL) [20,21].

of 2.2, 2.35 and 2.5 and analyzed for their carbon contents. Table 3 presents the result of the residual carbon content for the three different nitride specimens. The residual carbon content increases by increasing the graphite amount in the initial powder mixture. Also, the selected time and temperature of the reaction in this study (3 h and 1923 K) were not sufficient for complete removal of carbon in the nitride specimens. Arai et al. [19] reported that in order for carbon content to be less than 1000 ppm, residual carbon removal should use a time longer than 20 h at a temperature of 1823 K in an Ar+8 vol%H_2 atmosphere. Elimination of Ba and Sr contents, which is an important feature of fuel re-fabrication from spent fuel, was examined by chemical analysis of the elements and the results are shown in Table 4. After the preparation of the simulated spent oxide powder, the Ba and Sr contents are 1080 ppm and 418 ppm, respectively and, after nitration, the contents of both elements were reduced to less than 5 ppm, indicating that during the nitration reaction, most of these two elements can be eliminated.

The final sintered density of the nitride pellet obtained after sintering with the experimental conditions described in Section 2 and shown in Fig. 2 (at 1973 K, for 10 h and in Ar–4 vol%H_2 gas mixture) was about 80% TD (theoretical density). This is calculated by assuming the theoretical density of the re-fabricated simulated nitride containing fission product elements is 99% of the theoretical density of pure uranium mononitride (14.33 g/cm^3), based on the result that the theoretical density of a spent oxide fuel pellet is about 98.9% of the theoretical density of pure UO_2 [20]. Fig. 5 shows the microstructure of a re-fabricated nitride pellet using simulated spent oxide fuel, revealing that a larger number of pores exist in the inner part of the pellet rather than near the surface of the pellet.

Thermal diffusivity and specific heat were measured with the re-fabricated nitride specimens of 80% TD sintered density in the temperature range 295–373 K in an Ar atmosphere. The thermal conductivity was calculated from the measured values of the thermal diffusivity and specific heat of the specimens using the following relationship:

$$\lambda = \alpha \times cp \times \rho \tag{2}$$

where λ is the thermal conductivity, α the thermal diffusivity, cp the specific heat and ρ the density. In Fig. 6 the thermal conductivity of the re-fabricated nitride specimen was compared with other relevant fuel materials. It shows higher values than for UO_2 and the simulated spent oxide with densities of about 100%TD but lower values than for the pure uranium mononitride [20,21]. The difference in thermal conductivity between pure UO_2 and simulated spent oxide containing the fission products leads to the extrapolation that the simulated nitride specimen containing fission products has lower thermal conductivity than the pure uranium mononitride.

4. Conclusions

The nitration reaction behavior was investigated by use of a simulated fuel technique (SFT). Starting with a simulated spent nuclear oxide fuel, carbothermic reduction produced powder and, with the selected process parameters, simulated nitride fuel specimens were re-fabricated. These were characterized in terms of their phase, microstructure and density, and their compositional change and thermal conductivity.

In the nitration behavior study, it was observed that the nitration reaction rate was decreased for the simulated spent oxide compared with pure UO_2, due to the fission products which hindered the reaction rate. By re-fabrication of the simulated nitride specimens, it was judged that most of the process parameters in preparing pure uranium mononitride through carbothermic reduction can be adapted for re-fabricating nitride fuels from spent oxide fuel. Chemical analysis after the nitration and re-fabrication of the nitride pellet specimens revealed that the amounts of Ba and Sr elements were considerably reduced by the heat treatments during the reaction and sintering of the nitride pellet, implying that the process might be utilized for separation of certain fission products during a re-fabrication of nitride fuel for an advanced fuel cycle. Measurement and comparison of the thermal conductivity for the re-fabricated nitride specimens with other similar nuclear fuel materials revealed a higher thermal conductivity than for oxide fuel but lower than for pure uranium nitride.

Acknowledgement

This study has been performed by the support of one of the KAERI Projects.

References

[1] L.C. Walters, D.L. Porter, D.C. Crawford, Prog. Nucl. Energy 40 (2002) 513.
[2] D.C. Crawford, D.L. Porter, S.L. Hayes, J. Nucl. Mater. 371 (2007) 202.
[3] Ho Jin Ryu, Jae Won Lee, Young Woo Lee, Jung Won Lee, Geun Il Park, J. Korean Powder Metall. Inst. 15 (2008) 87.
[4] K. Minato, M. Akabori, M. Takano, Y. Arai, K. Nakajima, A. Itoh, T. Ogawa, J. Nucl. Mater. 320 (2003) 18.
[5] Y. Arai, K. Minato, J. Nucl. Mater. 344 (2005) 180.
[6] X.-C. Ding, T. Suzuki, T.M. Nomura, M. Aida, Y. Fujii, Prog. Nucl. Energy 47 (2005) 420.
[7] X.-C. Ding, T. Kaneshiki, M. Arima, M. Nomura, T. Suzuki, Y. Fujii, Prog. Nucl. Energy 50 (2008) 504.
[8] F. Kobayashi, T. Ogawa, M. Takano, M. Akabori, A. Itoh, K. Minato, S. Takahashi, in: Proceedings of International Conference on Global-99, Jackson Hole, Wyoming, 29 August–3 September 1999, CD-ROM.
[9] Hj. Matke, Science of Advanced LMFBR Fuels, North-Holland, Amsterdam, 1986.
[10] H. Blank, in: B.R.T. Frost (Ed.), Materials Science and Technology in Nuclear Materials, vol. 10A, VCH, Weinheim, 1994.
[11] IAEA-TECDOC-1374, Development status of metallic, dispersion and non-oxide advanced and alternative fuels for power and research reactors, International Atomic Energy Agency, Vienna, 2003.
[12] Fuels and Materials for Transmutation, NEA No. 5419, ISBN 92-64-01066-1, OECD/NEA, Paris, Chapter 2, 2005.
[13] Fuels and Materials for Transmutation, NEA No. 5419, ISBN 92-64-01066-1, OECD/NEA, Paris, Chapter 3, 2005.
[14] M.S. Yang, H. Choi, C.J. Jeong, K.C. Song, J.W. Lee, G.I. Park, H.D. Kim, W.I. Ko, J.J. Park, K.H. Kim, H.H. Lee, J.H. Park, Nucl. Eng. Tech. 38 (2006) 359.
[15] J.W. Lee, W.K. Kim, J.W. Lee, G.I. Park, M.S. Yang, K.C. Song, J. Nucl. Sci. Technol. 44 (2007) 597.
[16] P.G. Lucuta, Hj. Matzke, R.A. Verall, J. Nucl. Mater. 178 (1991) 48.
[17] A.G. Croff, Nucl. Technol. 62 (1983) 335.
[18] K.H. Kang, S.H. Na, K.C. Song, S.H. Lee, S.W. Kim, Thermochim. Acta 455 (2007) 129.
[19] Y. Arai, S. Fukushima, K. Shiozawa, M. Handa, J. Nucl. Mater. 168 (1989) 280.
[20] P.G. Lucuta, Hj. Matzke, R.A. Verall, J. Nucl. Mater. 217 (1994) 279.
[21] Y. Aral, K. Nakajima, Y. Suzuki, J. Alloys Compds. 271–273 (1998) 602.